High-spin properties of ^{164}Er in the multiple band crossing region

S. W. Yates
University of Kentucky, Lexington, Kentucky 40506
and Oak Ridge National Laboratory, Oak Ridge, Tennessee 37830

I. Y. Lee,* N. R. Johnson, and E. Eichler†
Oak Ridge National Laboratory, Oak Ridge, Tennessee 37830

L. L. Riedinger, M. W. Guidry,* and A. C. Kahler‡
University of Tennessee, Knoxville, Tennessee 37916
and Oak Ridge National Laboratory, Oak Ridge, Tennessee 37830

D. Cline*
Nuclear Structure Research Laboratory, University of Rochester, Rochester, New York 14627

R. S. Simon,§ P. A. Butler,‖ P. Colombani,¶ F. S. Stephens, and R. M. Diamond
Lawrence Berkeley Laboratory, University of California, Berkeley, California 94720

R. M. Ronningen,** R. D. Hichwa,†† and J. H. Hamilton
Vanderbilt University, Nashville, Tennessee 37235

E. L. Robinson
University of Alabama in Birmingham, Birmingham, Alabama 35294
(Received 31 October 1979)

High-spin states in ^{164}Er have been studied by using the ^{150}Nd(^{18}O,4$n\gamma$) and ^{164}Dy(α,4$n\gamma$) reactions and by multiple Coulomb excitation with ^{136}Xe ions. Several positive-parity bands are excited, and two negative-parity bands have been identified. The previously reported backbending behavior of the yrast sequence is demonstrated to result from the intersection of the ground band (seen to spin 22^+) with an even-spin "superband" observed from spins 12^+ to 24^+. The odd-spin yrast superband and the second lowest even-spin superband also have been observed. All the superbands have moments of inertia appreciably larger than the ground band. The observed intersection of these multiple superbands with the γ band produces different backbending behavior and a staggering of the energies of the odd- and even-spin members of the γ band. $B(E2)$ values for transitions below and through the band intersection regions of both the ground band and γ bands have been deduced from multiple Coulomb excitation yields. In addition, lifetimes have been measured for the ground band by the Doppler-broadened line-shape technique. The level energies and $B(E2)$ values are consistent with weak interaction matrix elements ($\approx$45 keV) between the intersecting bands. The $B(E2)$ values of the unperturbed band are found to obey the simple rigid-rotor relationship. The 7^- negative-parity band exhibits a normal rotational sequence, while the 5^- band exhibits a large odd-even staggering and a larger moment of inertia. Two-quasiparticle-plus-rotor model calculations indicate strong rotation-alignment and reproduce the observed properties of the high-spin states for both the positive- and negative-parity bands in ^{164}Er.

[NUCLEAR REACTIONS ^{150}Nd(^{18}O,4$n\gamma$), E=69.6 MeV, ^{164}Dy(α,4$n\gamma$), E=51 MeV, ^{164}Er(^{136}Xe,^{136}Xe$'\gamma$), E=547, 612, 620 MeV; measured E_γ, I_γ, $\gamma\gamma$ coin, Doppler-broadened line shapes, multiple Coulomb excitation probabilities; deduced levels, J, π, τ, $B(E2)$ values from lifetimes and yields, compared levels and $B(E2)$'s to theory.]

I. INTRODUCTION

The observed anomalous behavior of the moment of inertia at high spin in nuclear rotational bands (commonly referred to as backbending) is generally believed to be a result of the intersection of the ground-state rotational band with a second rotational band, i.e., the so-called yrast superband. The structure of this yrast superband, which has a moment of inertia close to the rigid-body value, has been interpreted primarily in terms of the rotation-alignment model[1,2] or the Coriolis antipairing model.[3] The rotation-alignment model attributes the structure of this superband to two high-j quasiparticles which are aligned with respect to the rotating core by the Coriolis force, while in the Coriolis antipairing formalism this band results from the collapse of

pairing.

Recent studies of the properties of both even- and odd-mass nuclei in the erbium region have provided an abundance of data which are in agreement with the predictions of the rotation-alignment model. Studies[4-6] of level energies and $B(E2)$ values of ^{164}Er through the backbend show behavior in reasonable agreement with the predictions of this model. The generalized calculations of Flaum and Cline[7] within the framework of the two-quasiparticle-plus-rotor model[1,2] predict not only the lowest superband, responsible for backbending, but also additional rotation-aligned bands of both positive and negative parity with similar moments of inertia at slightly higher excitation energies than the yrast superband. Experimental data relating to these additional bands and to the extension of known bands are, therefore, important to an understanding of high-spin nuclear structure. Data in the band-crossing region are particularly crucial, since they specify the interaction between the ground and γ bands with the superbands and hence, give information on the structure of the superband.

This paper details our previous studies[4-6] of ^{164}Er by the $(^{18}O, 4n\gamma)$, $(\alpha, 4n\gamma)$, and multiple Coulomb excitation reactions and presents new information on the $E2$ properties of the ground band and γ band derived from the Coulomb excitation data and new Doppler-broadened line-shape measurements. The advantages of such a combined set of measurements is apparent, if a truly extensive characterization of the high-spin states is sought. The determination of reduced transition probabilities from multiple Coulomb excitation, which selectively excites collective bands strongly coupled to the ground state, and from lifetimes measured by the Doppler-broadened line-shape method is important, because these quantities provide rigorous tests of nuclear models. The observed properties of the high-spin states in ^{164}Er are compared with the rotation-alignment model. We point out that our results are in quite good agreement with the recent study of ^{164}Er by Kistner, Sunyar, and der Mateosian.[8]

II. EXPERIMENTAL PROCEDURES AND RESULTS

A. In-beam γ-ray measurements

Gamma-ray measurements were performed at the Lawrence Berkeley Laboratory with the ^{164}Dy $(\alpha, 4n\gamma)^{164}$Er reaction and at Oak Ridge National Laboratory with the ^{150}Nd$(^{18}O, 4n\gamma)^{164}$Er reaction. While the results from the $(\alpha, 4n\gamma)$ reaction were instrumental in establishing the level structure in the backbending region of ^{164}Er, the more extensive $(^{18}O, 4n\gamma)$ measurements were used primarily in constructing the level scheme shown in Fig. 1 and will be described in greater detail.

A 2.8 mg/cm^2 self-supporting enriched neodynium foil (96% ^{150}Nd) was bombarded with 10–20 nA beams of 69.6-MeV ^{18}O ions from the Oak Ridge Isochronous Cyclotron (ORIC). Two large-volume (10% and 18% efficient for a 1.33-MeV γ ray relative to a 7.6 × 7.6 cm NaI(Tl) detector at 25 cm distance) Ge(Li) detectors having resolutions of 2.1 and 2.4 keV, respectively, were placed at 90° to the beam direction. Absorbers consisting of 0.28 mm of copper and 0.15 mm of tin were placed between the target and the detectors to reduce the number of x rays detected. The target to detector distance was 5 cm for the smaller detector and 7 cm for the larger detector.

Both γ-ray singles and γ-γ-time coincidence data (total of 3.5×10^7 coincidence events) were recorded simultaneously using a Tennecomp TP-5000 data acquisition system. The three-parameter coincidence data were stored serially on magnetic tape and prompt coincidences were later sorted using the same data system. Figure 2 shows a portion of the γ-ray singles spectrum, while Figs. 3 and 4 display some of the γ-γ coincidence spectra which are important in making level placements in the positive-parity bands. Gamma rays resulting from the Coulomb excitation of the ^{150}Nd target and, to a much lesser degree, from the production of ^{163}Er by the $(^{18}O, 5n\gamma)$ reaction are also present in the singles spectrum. Table I gives the energies, intensities, and placements of transitions which have been attributed to ^{164}Er. In many cases where the γ-ray singles spectrum was complex, energies and intensities were obtained from the coincidence spectra.

Analysis of the γ-ray spectra was performed with the interactive peak fitting codes PKFT (Ref. 9) and LIZA (Ref. 10) at Oak Ridge National Laboratory. The level scheme shown in Fig. 1 was constructed from our γ-ray measurements. The established spin assignments are based primarily on previous measurements,[8,11-15] while most levels with spins shown in parentheses are assigned on the basis of our coincidence information and γ-ray intensity values.

Recently, Kistner *et al.*[8] published their study of ^{164}Er from the ^{160}Gd$(^9Be, 5n\gamma)$ reaction which includes angular distribution and linear polarization measurements. Our level schemes are in quite good agreement; and, where discrepancies exist, they will be noted in the description which follows. Moreover, to first order it can be assumed that a similar degree of alignment is achieved in both the $(^{18}O, 4n)$ and $(^9Be, 5n)$ reac-

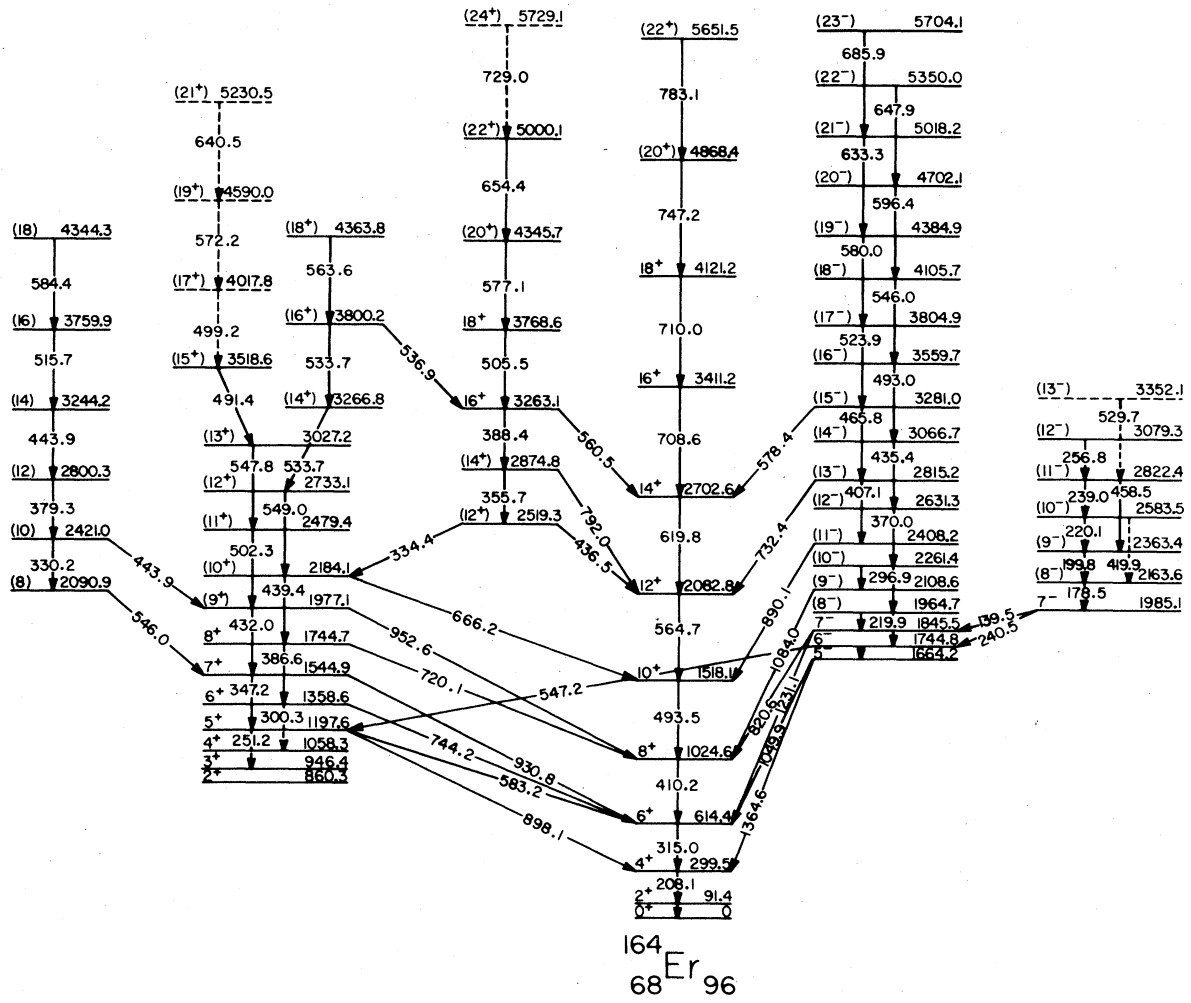

FIG. 1. Level scheme of ^{164}Er showing states populated by the ^{150}Nd(^{18}O, $4n$)^{164}Er reaction.

tions. This is verified by the fact that the relative intensities for the high-spin states are similar from the two reactions and, hence, the maximum angular momenta imparted in the two reactions are comparable. Thus, the γ-ray intensities listed in Table I include a $\lesssim 30\%$ correction for the angular distribution, which was calculated using the angular distribution data of Kistner *et al.*[8]

1. *The ground-state band*

Using in-beam γ-ray measurements, Jett and Lind[16] studied the levels of ^{164}Er populated by four different reactions and proposed levels in the ground-state rotational band to spin 14^+ on the basis of the agreement of observed with calculated γ-ray energies. Their assignments were confirmed by Banaschik *et al.*[11] who used the $(\alpha, 4n\gamma)$ reaction and by Davidson *et al.*[12] who employed not only the $(\alpha, 4n\gamma)$ reaction but also the $(^{14}\mathrm{C}, 4n\gamma)$ reaction for population of ^{164}Er levels. The coincidence and angular distribution measurements of the latter two studies[11,12] clearly showed that the levels up to the backbend in the ground-state band of Fig. 1 are connected by stretched $E2$ transitions.

Evidence for placement of the spin 16^+ and 18^+ members of the ground-state band came first from our ^{136}Xe induced Coulomb excitation data reported earlier.[4] The yield of the 709-keV (708.6 and 710.0 keV from our latest measurements) self-coincident doublet, which was placed as feeding the 14^+ state at 2703 keV, was observed to have 1.5 times the calculated yield for Coulomb excitation of the 16^+ state of the ground-state band. However, the predicted sum of the yields of the $18^+ \rightarrow 16^+$ and $16^+ \rightarrow 14^+$ transitions is in excellent agreement with the observed yield of this doublet, if rigid-rotor $B(E2)$ values are assumed. All the

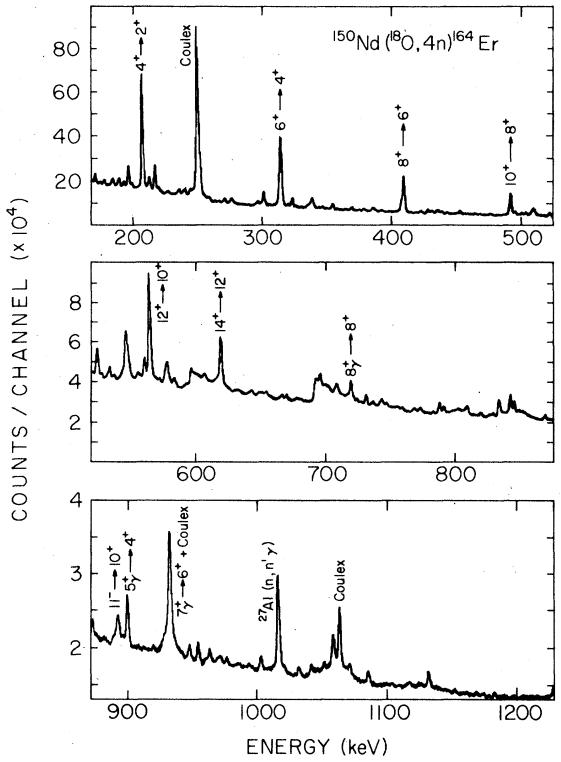

FIG. 2. Spectrum of γ rays observed following the ^{150}Nd(^{18}O, $4n$)^{164}Er reaction. Some of the more prominent peaks in the spectrum are labeled. Coulex refers to the Coulomb excitation of the ^{150}Nd target.

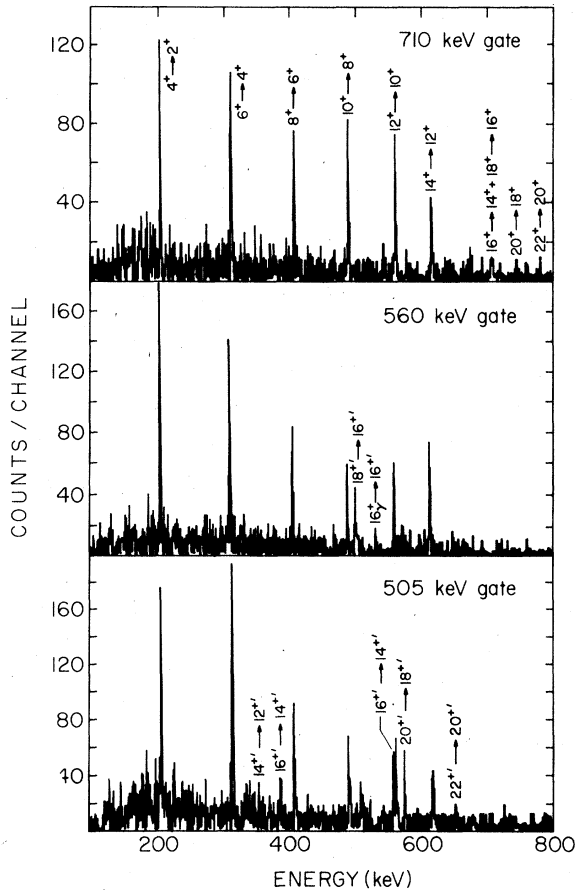

FIG. 3. Coincidence spectra from the 505-, 560-, and 710-keV gating transitions. Some of the more prominent peaks in the spectra are labeled.

available evidence, including our coincidence measurements (see Fig. 3), supports the proposed assignment.

The coincidence spectra also show transitions of 747.2 and 783.1 keV to be in coincidence with the 709-keV doublet. The energies and intensities of these γ rays suggest that they deexcite the next two members of the ground-state rotational band of ^{164}Er.

2. *The even-spin yrast superband*

The backbending of the yrast sequence in ^{164}Er was first observed by Banaschik *et al.*[11] who placed the 560.5-keV transition from the 16^+ state in the even-spin yrast superband to the 14^+ ground-band state. The yrast superband was extended to the 18^+ member at 3768.6 keV by Davidson *et al.*[12] and, on the basis of our (^{18}O, $4n\gamma$) coincidence measurements, the 20^+ and 22^+ levels have been assigned. Kistner *et al.*[8] have suggested that the 24^+ level is deexcited by a 729-keV γ-ray transition. This placement appears to be in agreement with our coincidence results, although the counting statistics of our coincidence data are only sufficient for us to make a tentative assignment.

The spin 14^+ level in the yrast superband was established on the basis of the observed coincidence of the 792-keV γ ray with the 565-keV γ ray ($12^+ \rightarrow 10^+$) in the ground-state band, the 388–792 keV γ-ray coincidence, and the excellent energy summation to the 3262.1-keV state via both decay paths. The branching ratio from the 16^+ yrast state is a sensitive measure of the interaction matrix element between the superband and ground-state band. Since the 388-keV region is complex in our singles spectrum, the intensity of the 388-keV γ ray was extracted from the coincidence spectra. The 388/560-keV γ-ray intensity ratio from our work, 0.22 ± 0.07, is not in good agreement with the value of 0.40 obtained from the study by Kistner *et al.*,[8] although no uncertainties are assigned to their γ-ray intensities.

The level at 2519 keV, which is placed from the observed coincidence with γ rays deexciting the 12^+ ground-band state, the 10^+ member of the γ-vibrational band (see next subsection), and the 14^+

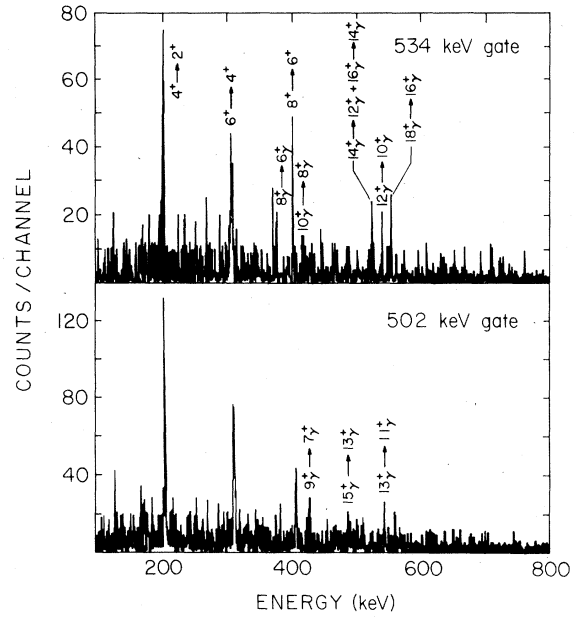

FIG. 4. Coincidence spectra from the 502- and 534-keV gating transitions. These data are from only one detector and have not been smoothed or summed. Some of the more prominent peaks in the spectra are labeled.

member of the yrast superband, is interpreted as the 12^+ member of the yrast superband. This assignment is in agreement with Kistner *et al.*[8] and, in addition, they report a 1001-keV γ ray which deexcites this state to the 10^+ ground-band state. A γ ray of this energy is clearly evident in our γ-ray singles spectrum, but its placement could not be made from our coincidence data. For this reason the transition from the 12^+ yrast superband state to the 10^+ member of the ground-state band is not included in our level scheme.

3. *The γ-vibrational band*

The γ-vibrational band of ^{164}Er has been established to spin 8^+ from studies of the β decay of the ^{164}Tm isomers[13] and from the in-beam spectroscopic work of Graetzer *et al.*[14] and West *et al.*[15] Our data are in agreement with these assignments. Although only weak evidence exists for population of the states having spins less than 5^+, these levels are well known and, for completeness, are shown in the level scheme. The even-spin members of the γ band are clearly seen in the Coulomb excitation data described in Sec. II B. The higher-spin levels shown in Fig. 1 were placed on the basis of our coincidence information and γ-ray intensity values.

When the backbending phenomenon was observed[6] in this γ-vibration band, considerable effort was expended in extending this band as far as possible. To this end, the coincidence gates

TABLE I. Energies, intensities, and assignments of γ rays observed in the ^{150}Nd(^{18}O, $4n\gamma$)^{164}Er reaction.

Energy[a] (keV)	Relative intensity[a,b] Exp.[c]	Corrected[d]	Transition[e] ($I^\pi_{\text{initial}} \rightarrow I^\pi_{\text{final}}$)
91.37 (6)	26 (2)		$2^+ \rightarrow 0^+$
118.7 (2)	1.4 (6)		$8^- \rightarrow 7^-$
139.5 (2)	1.6 (5)		$7^{-\prime} \rightarrow 7^-$
152.70 (12)	0.9 (2)	0.8 (3)	$10^- \rightarrow 9^-$
178.48 (6)	3.6 (2)	3.4 (2)	$8^{-\prime} \rightarrow 7^{-\prime}$
199.75 (9)	3.5 (3)	3.3 (3)	$9^{-\prime} \rightarrow 8^{-\prime}$
208.10 (6)	100	100	$4^+ \rightarrow 2^+$
219.9 (2)	2.0 (8)		$8^- \rightarrow 6^-$
220.1 (2)	2.5 (6)		$10^{-\prime} \rightarrow 9^{-\prime}$
239.0 (3)	1.8 (4)	1.7 (4)	$11^{-\prime} \rightarrow 10^{-\prime}$
240.5 (1)	4.8 (3)	4.4 (3)	$7^{-\prime} \rightarrow 6^-$
251.2	<0.5		$(5^+_\gamma \rightarrow 3^+_\gamma)$
256.8 (4)	0.6 (3)	0.6 (3)	$12^{-\prime} \rightarrow 11^{-\prime}$
296.93 (7)	4.7 (3)	4.7 (3)	$10^- \rightarrow 8^-$
300.3	<0.5		$(6^+_\gamma \rightarrow 4^+_\gamma)$
314.95 (7)	88 (5)	88 (5)	$6^+ \rightarrow 4^+$
330.2 (2)	1.3 (2)		$10 \rightarrow 8$
334.4 (4)	2.2 (9)		$12^{+\prime} \rightarrow 10^+_\gamma$
347.2 (2)	2.2 (3)		$7^+_\gamma \rightarrow 5^+_\gamma$
355.7 (4)	0.7 (3)		$14^{+\prime} \rightarrow 12^{+\prime}$
369.96 (6)	4.4 (2)	4.6 (3)	$12^- \rightarrow 10^-$
379.32 (7)	2.2 (2)	2.2 (2)	$12 \rightarrow 10$
386.6 (4)	2.3 (9)	2.3 (9)	$8^+_\gamma \rightarrow 6^+_\gamma$
388.4 (3)	1.1 (3)	1.1 (3)	$16^{+\prime} \rightarrow 14^{+\prime}$
407.1 (4)	1.3 (7)	1.3 (7)	$13^- \rightarrow 11^-$
410.22 (7)	65 (5)	67 (5)	$8^+ \rightarrow 6^+$
419.9 (6)	0.2 (2)		$(10^{-\prime} \rightarrow 8^{-\prime})$
431.95 (7)	4.7 (3)	4.9 (4)	$9^+_\gamma \rightarrow 7^+_\gamma$
435.4 (3)	3.2 (5)	3.3 (5)	$14^- \rightarrow 12^-$
436.5 (5)	2.6 (4)	2.7 (4)	$12^{+\prime} \rightarrow 12^+$
439.43 (8)	2.6 (3)	2.6 (3)	$10^+_\gamma \rightarrow 8^+_\gamma$
443.9 (2)	2.9 (3)		$14 \rightarrow 12$ $10 \rightarrow 9^+_\gamma$
458.5 (4)	1.7 (9)		$11^{-\prime} \rightarrow 9^{-\prime}$
465.8 (1)	2.1 (2)	2.1 (2)	$15^- \rightarrow 13^-$
491.4 (4)	1.4 (6)		$15^+_\gamma \rightarrow 13^+_\gamma$
493.0 (3)	1.3 (4)		$16^- \rightarrow 14^-$
493.46 (10)	52 (3)	54 (3)	$10^+ \rightarrow 8^+$
499.2 (4)	1.1 (6)	1.1 (6)	$(17^+_\gamma \rightarrow 15^+_\gamma)$

TABLE I. (*Continued.*)

Energy [a] (keV)	Relative intensity [a,b] Exp. [c]	Corrected [d]	Transition [e] ($I^{\pi}_{\text{initial}} \rightarrow I^{\pi}_{\text{final}}$)
502.33 (6)	3.2 (2)	3.3 (2)	$11^{+}_{\gamma} \rightarrow 9^{+}_{\gamma}$
505.50 (6)	4.7 (3)	4.8 (4)	$18^{+\prime} \rightarrow 16^{+\prime}$
515.7 (3)	1.1 (4)	1.1 (4)	$16 \rightarrow 14$
523.9 (4)	3.8 (10)	3.9 (11)	$17^{-} \rightarrow 15^{-}$
529.7 (4)	0.9 (5)		$(13^{-\prime} \rightarrow 11^{-\prime})$
533.7 (3)	2.9 (2)		$16^{+}_{\gamma} \rightarrow 14^{+}_{\gamma}$
			$14^{+}_{\gamma} \rightarrow 12^{+}_{\gamma}$
536.9 (3)	1.8 (8)		$16^{+}_{\gamma} \rightarrow 16^{+\prime}$
546.0 (5)	1.0 (4)		$18^{-} \rightarrow 16^{-}$
546.0 (5)	1.5 (6)		$8 \rightarrow 7^{+}_{\gamma}$
547.2 (4)	5.1 (13)		$6^{-} \rightarrow 5^{+}_{\gamma}$
547.8 (4)	2.2 (9)		$13^{+}_{\gamma} \rightarrow 11^{+}_{\gamma}$
549.0 (4)	2.3 (8)	2.3 (8)	$12^{+}_{\gamma} \rightarrow 10^{+}_{\gamma}$
560.50 (11)	4.9 (5)	5.1 (5)	$16^{+\prime} \rightarrow 14^{+}$
563.6 (5)	1.7 (9)		$18^{+}_{\gamma} \rightarrow 16^{+}_{\gamma}$
564.73 (6)	32 (2)	33 (2)	$12^{+} \rightarrow 10^{+}$
572.2 (2)	1.1 (6)		$(19^{+}_{\gamma} \rightarrow 17^{+}_{\gamma})$
577.1 (3)	1.9 (5)	2.0 (5)	$20^{+\prime} \rightarrow 18^{+\prime}$
578.4 (6)	1.2 (6)	1.0 (6)	$15^{-} \rightarrow 14^{+}$
580.0 (2)	2.3 (6)	2.3 (7)	$19^{-} \rightarrow 17^{-}$
583.2 (2)	2.1 (3)		$5^{+}_{\gamma} \rightarrow 6^{+}$
584.4 (4)	1.0 (3)		$18 \rightarrow 16$
596.4 (3)	0.7 (3)	0.7 (3)	$20^{-} \rightarrow 18^{-}$
619.76 (11)	16 (2)	17 (2)	$14^{+} \rightarrow 12^{+}$
633.3 (4)	1.7 (9)	1.7 (9)	$21^{-} \rightarrow 19^{-}$
640.5 (4)	1.1 (6)		$(21^{+}_{\gamma} \rightarrow 19^{+}_{\gamma})$
647.9 (4)	0.7 (3)		$22^{-} \rightarrow 20^{-}$
654.4 (4)	1.6 (2)	1.6 (3)	$22^{+\prime} \rightarrow 20^{+\prime}$
666.2 (2)	1.6 (10)		$10^{+}_{\gamma} \rightarrow 10^{+}$
685.9 (8)	1.7 (9)		$23^{-} \rightarrow 21^{-}$
708.6 (3)	2.7 (5)	2.8 (6)	$16^{+} \rightarrow 14^{+}$
710.0 (3)	2.5 (5)	2.6 (6)	$18^{+} \rightarrow 16^{+}$
720.1 (2)	2.3 (10)	1.8 (9)	$8^{+}_{\gamma} \rightarrow 8^{+}$
729.0 (5)	0.4 (2)		$(24^{+\prime} \rightarrow 22^{+\prime})$
732.4 (1)	3.4 (4)	2.6 (4)	$13^{-} \rightarrow 12^{+}$
744.2 (3)	4.4 (15)	3.6 (13)	$6^{+}_{\gamma} \rightarrow 6^{+}$
747.2 (4)	1.4 (4)		$20^{+} \rightarrow 18^{+}$
783.1 (4)	0.8 (3)		$22^{+} \rightarrow 20^{+}$
791.98 (7)	3.0 (2)	3.1 (3)	$14^{+\prime} \rightarrow 12^{+}$
820.6 (2)	1.6 (3)		$7^{-} \rightarrow 8^{+}$
890.12 (11)	3.5 (3)	2.7 (3)	$11^{-} \rightarrow 10^{+}$
898.14 (6)	7.6 (4)	6.4 (4)	$5^{+}_{\gamma} \rightarrow 4^{+}$
930.8 (4)	4.4 (14)	3.4 (11)	$7^{+}_{\gamma} \rightarrow 6^{+}$
952.60 (7)	3.3 (3)	2.5 (3)	$9^{+}_{\gamma} \rightarrow 8^{+}$
1049.0 (9)	1.0 (2)	0.9 (2)	$5^{-} \rightarrow 6^{+}$
1083.95 (9)	2.1 (2)	1.7 (2)	$9^{-} \rightarrow 8^{+}$
1231.10 (7)	5.0 (3)	4.2 (3)	$7^{-} \rightarrow 6^{+}$
1364.6 (3)	3.9 (5)	3.3 (5)	$5^{-} \rightarrow 4^{+}$

[a] Uncertainties in the least significant figures are indicated in parentheses.

[b] Intensities are normalized to 100 for the 208.10-keV γ ray.

[c] Experimental singles values with Ge(Li) detector located at 90° with respect to the beam direction.

[d] The intensities have been corrected for the angular distribution effect using the experimental angular distribution coefficients of Kistner *et al.* (Ref. 8).

[e] The symbols used in transition placements can readily be understood by a comparison with the band structures shown in Fig. 1. Tentative γ-ray transition placements are indicated in parentheses.

providing information on this band were scanned with gates set on the first detector, and spectra were stored for the second detector. The gating was then done on the second detector, and spectra were recorded for the first detector. After the spectra were normalized for energy, they were summed. As a final aid in making decisions on the weak coincidences, the data were smoothed.

It is convenient to discuss the even-spin levels separately from the odd-spin levels, since there are no intraband transitions between these sets of levels. The even-spin sequence was extended to spin 18^{+}. The 534-keV γ-ray peak in the spectrum is a selfcoincident doublet and was assigned as the transitions deexciting the 16^{+} and 14^{+} levels of the γ-vibrational band on the basis of intensity. The observed 537-keV transition from the 16^{+} state to the 16^{+} yrast superband state lends further support to these placements. No even-spin states higher than the proposed 18^{+} state at 4363.8 keV could be extracted from our data.

As a result of the complexity of the γ-ray spectra, the 502-keV ($11^{+}_{\gamma} \rightarrow 9^{+}_{\gamma}$) transition is the highest-lying γ ray which can reliably be used as a gating transition in the odd-spin sequence. This coincidence spectrum shows the 548-keV and

the 491-keV γ rays in coincidence as well as γ rays at 499, 572, and 641 keV which have a coincidence intensity of ~80% of that of the 491-keV γ ray. We have suggested[6] that the latter three γ rays form a cascade into the 15^+ level. The level order is based on level systematics in the backbending region where abrupt changes have not been observed. Any order other than that shown produced a severe discontinuity in the backbending plot. Since these placements are tentative, they are shown as dashed in the level scheme. Kistner *et al.*[8] showed that the 499.2-keV $(17^+_\gamma - 15^+_\gamma)$ transition has the angular distribution of a stretched $E2$ transition, and they also observed a 571-keV γ ray, which they assigned as the $(19^+_\gamma - 17^+_\gamma)$ transition.

4. *The $K^\pi = 5^-$ band*

The first three members of the rotational band built on the 5^- state at 1664.2 keV have been assigned from the decay of $^{164}Tm^m$ by de Boer *et al.*[13] The 80-keV γ ray which depopulates the 6^- state has been reported[13] but was not seen in our measurements because of its large internal conversion coefficient and high probability of absorption. The coincidence data suggest, however, that this transition must exist. We also did not observe the 101-keV $(7^- \rightarrow 6^-)$ transition. The additional members of this band shown in Fig. 1 were established from the coincidence results.

Kistner *et al.*[8] have observed this band to spin 24. Our level scheme is in excellent agreement with theirs, but we have not been able to substantiate their placement of the highest state (24^-).

5. *The $K^\pi = 7^-$ band*

The 7^- state at 1985.1 keV has been assigned[13] as the $\{\frac{1}{2}^+[404]\pi; \frac{1}{2}^-[523]\pi\}_{7^-}$ state because of the observed allowed unhindered electron capture decay to this level from the 6^- isomeric state of ^{164}Tm. The γ rays from the levels of the rotational band built on this state are observed by gating on the 240-keV γ ray which most strongly deexcites the 7^- state into the aforementioned $I^\pi = 5^-$ negative-parity band. The regular rotational sequence of level energies and the observation of both cascade and cross-over transitions leaves little doubt as to the identity of the band up to spin 12^-. The 13^- level is placed solely on the basis of the coincidence of the 530-keV γ ray with the 239-keV γ ray and the energy systematics. Kistner *et al.*[8] also report a 273-keV γ ray from this level, but this transition could not be confirmed by our spectral measurements.

6. *The rotational band based on 2090.9 keV*

A series of states which form a band of unknown parity was placed by Kistner *et al.*[8] who suggested that the lowest observed level at 2091.3 keV had a spin of 8. Our work substantiates these placements up through the sixth member ($I=18$) of this band and their arguments about this band appear to be well based.

B. Multiple Coulomb excitation measurements

The nucleus ^{164}Er is one of the few stable nuclei which is known to exhibit backbending behavior. With very heavy ions such as ^{136}Xe it is possible to Coulomb excite ^{164}Er into the high angular momentum states of the backbending region with appreciable cross section. This is quite advantageous because Coulomb excitation selectively populates collective bands strongly coupled to the ground state as opposed to the γ-decay pattern following (HI, xn) reactions which is often constrained to follow the yrast sequence. Consequently, Coulomb excitation leads to much less complicated γ-ray spectra than those obtained using nuclear reactions. In addition, the γ-ray transition yields following Coulomb excitation can be used to establish the $B(E2)$ values.

The target used in the multiple Coulomb excitation measurements was a 1.34 mg/cm^2 isotopically enriched (73.6% ^{164}Er) metallic self-supporting erbium foil. This target was bombarded with 547- and 612-MeV ^{136}Xe ions from the Lawrence Berkeley Laboratory SuperHILAC, and the deexcitation γ rays were detected by a 50-cm^3 Ge(Li) detector. Silicon detectors were used to detect scattered Xe ions at angles of 65°, 77°, and 90° (three detectors at each angle) in coincidence with γ rays observed in the Ge(Li) detector at $-30°$ to the incident beam. By placing the Ge(Li) detector in the average recoil direction, where the Doppler shift is maximum (8%) and the Doppler broadening is minimum, and by correcting for the different recoil velocities occurring at different scattering angles, γ-ray energy resolution of $\leq 1\%$ full width at half maximum (FWHM) was achieved. A multiplicity filter consisting of four 7.6×7.6 cm NaI(Tl) detectors was used to determine the multiplicity of each γ-ray transition observed in the Ge(Li) spectrum in coincidence with scattered ions. The dependence of the γ-ray yields on (1) the multiplicity distribution, (2) the bombarding energy, and (3) the projectile scattering angle, provided three independent measures of the location of each deexciting γ-ray transition in the nuclear decay scheme. These confirmed the decay scheme derived from the $(^{18}O, 4n\gamma)$ reaction shown in Fig. 1.

A spectrum of γ rays in coincidence with scattered ^{136}Xe ions is shown in Fig. 5. A striking feature of this spectrum is that Coulomb excitation preferentially populates the extension of the ground band above the intersection with the lowest superband. Observed γ-ray transitions involving levels in both the ground-state band and γ band are indicated. Unmarked peaks are from Coulomb excitation of ^{166}Er or ^{168}Er contaminants or from excited target nuclei which recoil into the silicon detectors and exhibit a small Doppler shift. The yields for each γ-ray transition were obtained using an interactive peak fitting routine FIT.[17]

The Winther-de Boer[18] computer program, which assumes semiclassical Coulomb excitation theory, was used to calculate the γ-ray yields. The symmetric rotor model was used to calculate the $E2$ matrix elements with $\langle 0||M(E2)||2_1\rangle = 2.341\ e$ b, which is taken from α-particle Coulomb excitation measurements.[19] For simplicity we have used the rigid-triaxial-rotor model with $\gamma = 12.7°$ for the γ band. The matrix elements calculated with this small value for the asymmetry parameter should closely approximate those of rotation-vibration calculations. The two-band mixing model, using a 45-keV interaction strength, was used to estimate the $B(E2)$ values coupling the ground band and yrast even-spin superbands. The weak $B(E2; 2^+_\gamma \rightarrow 2^+)$, $B(E2; 8^+_\gamma \rightarrow 8^+)$, and $B(E2; 10^+_\gamma \rightarrow 10^+)$ matrix elements were adjusted slightly to ensure that the experimental branching ratios were obtained. The calculations also included $E4$ matrix elements derived assuming that $\langle 0||M(E4)||4_1\rangle = +0.12\ e\,\text{b}^2$ and assuming that only the Q_{40} intrinsic $E4$ moment is nonzero. The inclusion of $E4$ excitation produced $\lesssim 2\%$ changes in the calculated γ-ray yields. The calculations of the γ-ray yields included (1) $M1$ transition matrix elements derived from known $E2/M1$ mixing ratios[15] and systematics; (2) the deorientation effect ($\lesssim 20\%$ effect), calculated using the two-state model of Brenn *et al.*[20]; (3) the finite size of the Ge(Li) and summing effects in the Ge(Li) ($\simeq 1\%$ correction); and (4) internal conversion. These corrections are predicted reliably and accurately and are smaller than the uncertainties involved in obtaining the yields from the γ-ray spectra. The only important systematic error occurs for a bombarding energy of 612 MeV where we expect a small Coulomb-nuclear interference effect.[21] This slightly excessive bombarding energy was chosen in order to maximize the excitation probabilities through the band intersection region which was not fully explored when these Coulomb excitation data were reported.[4] It is estimated that the Coulomb-nuclear interference will produce $\lesssim 5\%$ uncertainty in the $B(E2)$ values extracted from the data taken at 612 MeV and is a negligible correction for the 547-MeV data.

A comparison of the experimental and calculated sums of γ-ray yields deexciting each level is shown in Fig. 6. The sum of the $18^+ \rightarrow 16^+$ and $16^+ \rightarrow 14^+$ unresolved doublet and also the sum of the

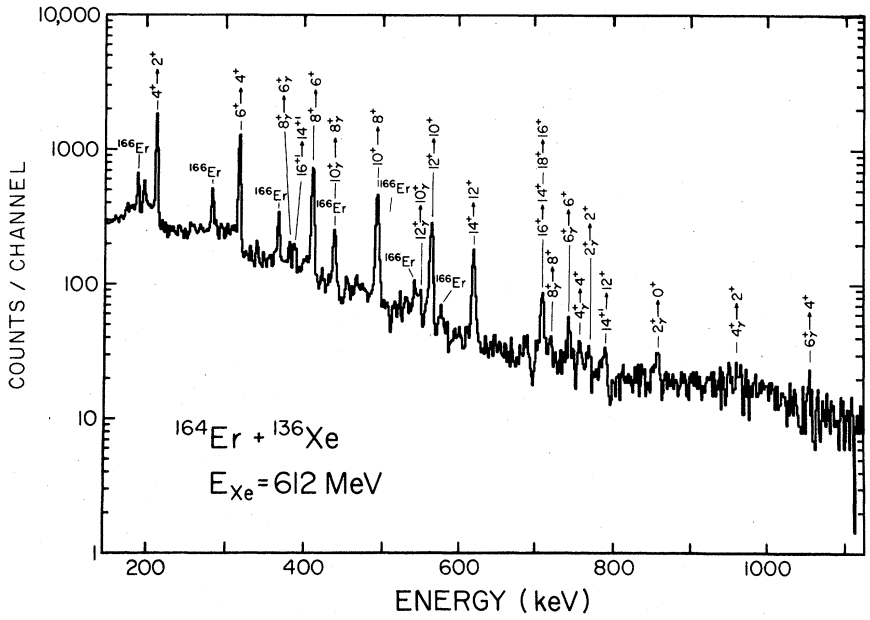

FIG. 5. Coincidence γ-ray spectrum for the Coulomb excitation of ^{164}Er by 612-MeV ^{136}Xe ions. Transitions in ^{164}Er are labeled.

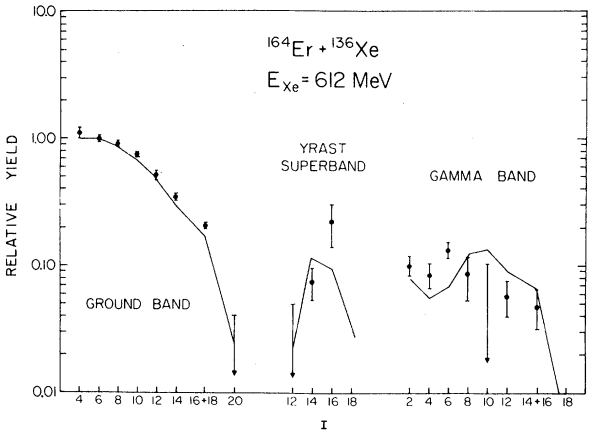

FIG. 6. Comparison of the total yield of γ rays from multiple Coulomb excitation of ^{164}Er by 612-MeV ^{136}Xe ions with Coulomb excitation calculations. The measured and calculated yield of the 16^+ state was corrected to include the known branching ratio.

$16^+_\gamma \rightarrow 14^+_\gamma$ and $14^+_\gamma \rightarrow 12^+_\gamma$ unresolved doublet are compared with the sum of the calculated yields of the unresolved transitions in Fig. 6. Destructive interference occurs for multiple Coulomb excitation of the odd-spin members of the γ band with the result that they are calculated to be populated ~20 times weaker than the adjacent even-spin γ-band states. The population of these odd-spin states is not shown in Fig. 6, since they are too weakly excited to be observed in the present work. Unfortunately, the even-spin yrast superband was difficult to observe because the $16^+ \rightarrow 14^+$ transition, which is the strongest branch from the 16^+ superband state, is not resolved from the strong $12^+ \rightarrow 10^+$ ground-band transition. The overall agreement between experiment and calculation is satisfactory for all three bands indicating that the assumed $E2$ properties are consistent with the data.

The extraction of individual $B(E2)$ values from the above comparison is somewhat complicated, since most states were populated by multistep excitation and thus the yield of a given state depends on several matrix elements. However, a large part of this complexity is removed by comparing the experimental and calculated ratios of γ-ray yields of successive levels connected by large $B(E2)$ values, i.e., for the ground band, the ratio $R_I = Y_I/Y_{I-2}$ where Y_I is the yield of γ rays deexciting the spin I state. The sensitivity of R_I to the $B(E2; I-2 \rightarrow I)$ can be expressed as

$$\frac{R_I^{\text{exp}} - R_I^{\text{calc}}}{R_I^{\text{calc}}} = \alpha_I \left[\frac{B(E2; I-2 \rightarrow I)_{\text{exp}} - B(E2; I-2 \rightarrow I)_{\text{calc}}}{B(E2; I-2 \rightarrow I)_{\text{calc}}} \right].$$

It can be shown[22] that the sensitivity parameter $\alpha_I \approx 1 - R_I$. The Coulomb excitation code[18] was used to calculate the coefficient α_I. The final $B(E2)$ values were obtained by an iterative procedure where the above relation was used to correct the $B(E2)$ values used in the initial calculations.

For the ground-band states up to spin 14^+, the experimental value of R_I is equal, within the 5–10% statistics, to the theoretical value of R_I

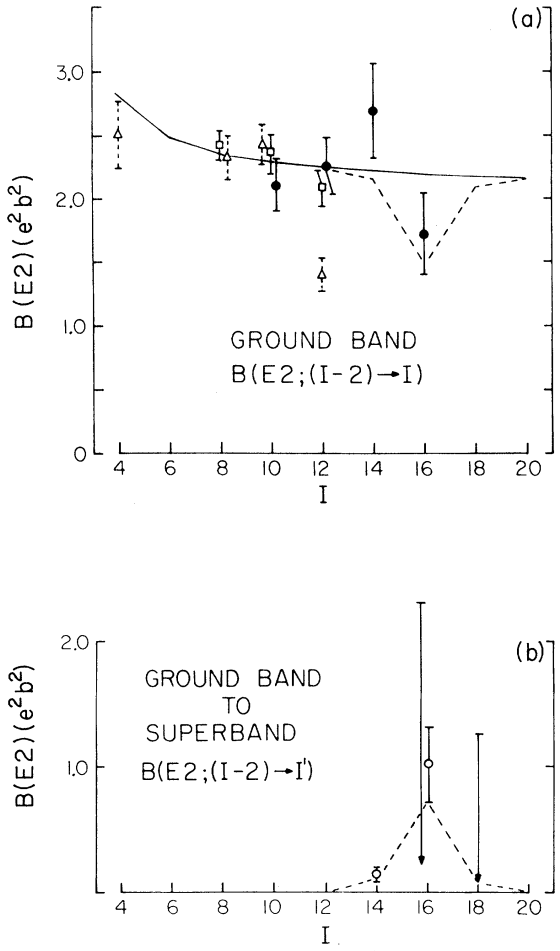

FIG. 7. $B(E2)$ values extracted for the Coulomb excitation yields (solid circles), Doppler-broadened line shape (open squares), and results from previous work (triangles). The solid line corresponds to the $B(E2)$ values derived from the $B(E2; 0^+ \rightarrow 2^+)$ assuming the rigid-spheroidal-rotor relation. The dashed line corresponds to the $B(E2)$ values derived assuming a 45-keV interaction matrix element between the intersecting bands and assuming identical intrinsic quadrupole moments for both bands. The open circles for the superband correspond to the $B(E2)$ values derived from the measured branching ratio assuming that the superband has a constant and similar intrinsic quadrupole moment to that of the ground band.

evaluated using the spheroidal rigid-rotor relation for the $B(E2)$ values. Although this implies that on the average the experimental $B(E2)$ values are close to the values derived from the known $B(E2;0^+ \rightarrow 2^+)$ assuming the rigid-rotor relation, it does not prove that the individual $B(E2)$ values obey this relation. Typically, α_I is less than 0.3 for transitions between ground-band states below $I^\pi = 12^+$. Consequently, the $B(E2)$ value derived from a given R_I has a fractional error magnified by a factor of more than three compared with the fractional error in R_I. Multiple Coulomb excitation data obtained with lower bombarding energies or with lighter projectiles would provide reliable $B(E2)$ values for ground-band states below spin 10^+.

The ground-band $B(E2)$ values extracted from the present multiple Coulomb excitation data are shown in Fig. 7 and listed in Table II. The individual ground-band $B(E2)$ values are consistent with the rigid-rotor relation (solid curve) amended to include band mixing (dashed curve). The ground to superband $B(E2)$ values are poorly determined by the Coulomb excitation data because, as mentioned earlier, the strongest branch from the $16^{+\prime}$ state was masked by the $(12^+ \rightarrow 10^+)$ ground-band transition. The dashed line corresponds to the $B(E2)$ values used in the Coulomb excitation calculations.

The $B(E2)$ values involving the γ band used in the Coulomb excitation calculations are indicated by the dashed lines in Fig. 8. The values are those given by the rigid-triaxial-rotor model except that the $B(E2;2^+_\gamma \rightarrow 2^+)$, $B(E2;8^+_\gamma \rightarrow 8^+)$, and $B(E2;10^+_\gamma \rightarrow 10^+)$ values were slightly adjusted to obtain better agreement with the known branching ratios. Both the intraband and interband $B(E2)$ values strongly influence the population of states in the γ band. This complication, coupled with the weak and uniform population of γ-band states up to spin 10^+, makes it possible to extract reliable $B(E2)$ values only for the unresolved $(16^+_\gamma \rightarrow 14^+_\gamma)$ and $(14^+_\gamma \rightarrow 12^+_\gamma)$ doublet and the $(12^+_\gamma \rightarrow 10^+_\gamma)$ transition. Within the very large error, these individual $B(E2)$ values are consistent with the model values.

C. Lifetimes from Doppler-broadened line-shape analysis

Heavy-ion Coulomb excitation is ideal for measuring lifetimes of excited states by the Doppler-broadened line-shape technique, because the recoil velocities are large and the population of states is well understood. The large recoil velocity $(v/c \approx 0.08)$ imparted by Xe projectiles makes this

TABLE II. Lifetimes and $B(E2)$ values for states in ^{164}Er.

Transition $I \rightarrow I-2$	Doppler-broadened line shape Meanlife τ_{exp} (ps)	$B[E2;\ I \rightarrow (I-2)]$ $(e\,b)^2$	Multiple Coulomb excitation $B[E2;\ I \rightarrow (I-2)]$ $(e\,b)^2$	Previous work $B[E2;\ I \rightarrow (I-2)]$ $(e\,b)^2$	Rigid rotor $B[E2;\ I \rightarrow (I-2)]$ $(e\,b)^2$
Ground band					
$4^+ \rightarrow 2^+$				1.39 ± 0.14 [a]	1.57
$6^+ \rightarrow 4^+$					1.73
$8^+ \rightarrow 6^+$	3.69 ± 0.18	1.86 ± 0.09		1.78 ± 0.13 [b]	1.81
$10^+ \rightarrow 8^+$	1.46 ± 0.09	1.91 ± 0.12	1.70 ± 0.16	1.96 ± 0.12 [b]	1.85
$12^+ \rightarrow 10^+$	0.8 ± 0.06	1.75 ± 0.13	1.89 ± 0.19	1.19 ± 0.09 [b]	1.89
$14^+ \rightarrow 12^+$			2.33 ± 0.32		1.91
$16^+ \rightarrow 14^+$			1.52 ± 0.28 [c]		1.93
Superband					
$16^{+\prime} \rightarrow 14^+$			≤2.8		
Gamma band					
$12^+_\gamma \rightarrow 10^+_\gamma$			1.5 ± 0.7		1.59
$14^+_\gamma \rightarrow 12^+_\gamma$			1.9 ± 0.9 [c]		1.62

[a] Reference 47—lifetime measurement by a microwave technique.

[b] Reference 29—Doppler-broadened line-shape measurement.

[c] Gamma ray unresolved from a weaker transition between next two higher members of the collective band. This quoted $B(E2)$ value was extracted assuming that the weaker transition from the higher transition was correctly calculated using a $B(E2)$ value given by the rotational model.

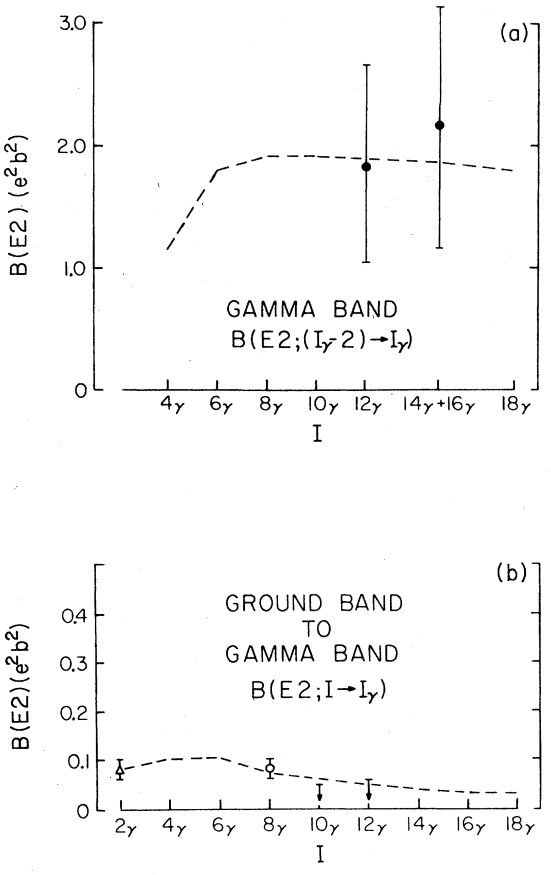

FIG. 8. The $B(E2)$ values for the γ band derived from the Coulomb excitation data. The dashed line corresponds to the values used in the calculation and was derived using the rigid-triaxial-rotor model as described in the text. The open circle for the $B(E2; 8^+ \rightarrow 8^+_\gamma)$ was derived from the branching ratio assuming that the intraband transitions were given by the rotor model.

technique a sensitive method for studying the short lifetimes characteristic of high-spin states. This method complements the multiple Coulomb excitation method for extracting $B(E2)$ values, because the present multiple Coulomb excitation yields are insensitive to the $B(E2)$'s of those lower-spin states which are most easily studied by Doppler-broadened line-shape analysis. In addition, complications involving the complex feeding patterns and feeding times, which make it difficult to measure lifetimes of states populated following (HI,xn) reactions, are avoided. Using this technique, we have performed lifetime measurements of the 8^+, 10^+, and 12^+ ground-band states in ^{164}Er.

A thick ~30 mg/cm^2 metallic ^{164}Er target was bombarded by a beam of 620-MeV ^{136}Xe ions from the Lawrence Berkeley Laboratory SuperHILAC. This target was of sufficient thickness to stop the beam and the recoiling ^{164}Er target nuclei. The deexcitation γ rays following Coulomb excitation were detected in a 50-cm^3 Ge(Li) detector placed at 0° to the beam. As can be seen in Fig. 9, the γ rays emitted during deceleration of the recoiling nuclei in the target are Doppler broadened. The lifetime of the state can be extracted from the shape of the γ-ray peak and a knowledge of the slowing-down time. The lineshapes of the γ rays from the $8^+ \rightarrow 6^+$, $10^+ \rightarrow 8^+$, and $12^+ \rightarrow 10^+$ transitions were analyzed using the computer code DOPCO.[23] In this code the recoil velocity and angular distribution of the target nucleus are taken together with the stopping power, and the expected lineshape for a given lifetime is calculated.

The angular distribution and the excitation function of the Coulomb excitation process were calculated using the program of Winther and de

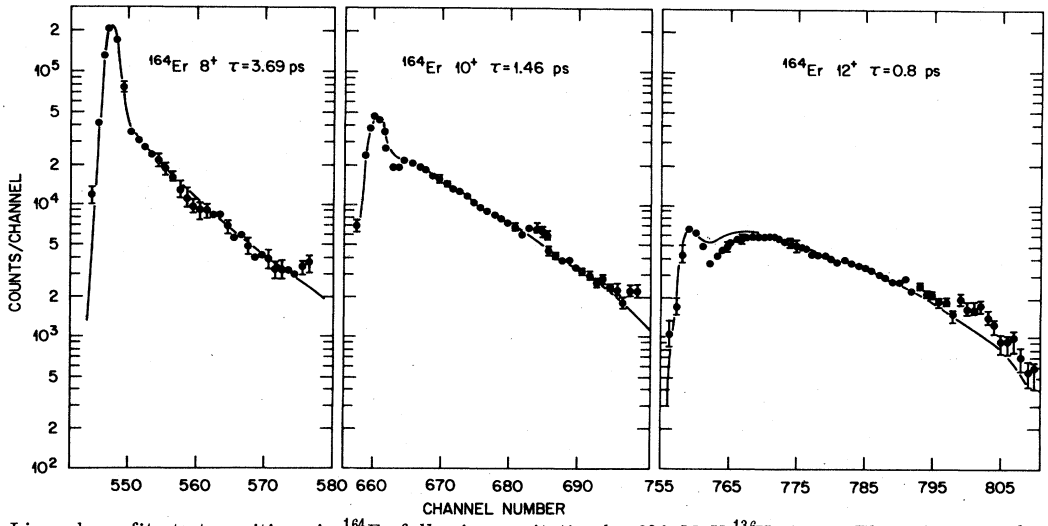

FIG. 9. Line-shape fits to transitions in ^{164}Er following excitation by 620-MeV ^{136}Xe ions. The points are the experimental data and the solid lines are the calculated fits from the program DOPCO (Ref. 23).

Boer.[18] The $E2$ and $E4$ matrix elements described in the previous section were used. Gamma-ray yields and angular distributions were calculated for center-of-mass particle scattering angles ranging from 20° to 180° in 20° steps at energies from 80 to 620 MeV in five steps to account for energy loss in the thick target.

The electronic stopping powers, taken from the table of Northcliffe and Schilling,[24] were corrected at low energies for medium dependences using the table of Ziegler and Chu[25] according to the usual procedure.[26] The maximum correction was found to be about 8%. The theory of Lindhard *et al.*[27] was used for the nuclear stopping powers, and the large-angle scattering effect was taken into account using the Blaugrund[28] prescription.

Lifetimes were obtained from a least squares fit of the calculated line shapes to the experimental data and are listed in Table II. The uncertainties include statistical contributions from the data, errors in background subtraction, and uncertainties in the stopping powers. The state of highest spin (12^+) was analyzed first; hence, the γ-ray feeding to the next lower state is treated properly by using the experimentally determined lifetime. Feeding from 14^+, 16^+, and 18^+ states were also included by assuming rotational lifetimes for these states.

The best fits to the γ-ray transitions depopulating the 8^+, 10^+, and 12^+ states are shown in Fig. 9. The region of the line shape just above the stopped component of the peak from the $12^+ \rightarrow 10^+$ transition is not well reproduced by the calculation. This may indicate that the values of the stopping power at low velocity ($v/c \sim 0.004$) are not correct in our calculations. However, the extracted lifetime is not very sensitive to this deviation because this region represents only a small fraction of the total counts. As a check of the integrity of our calculations, an analysis of this data was performed with a different computer code.[26] The results of these calculations were in excellent agreement with those presented in Table II.

The $B(E2)$ values derived from the measured lifetimes are in excellent agreement with the rigid-rotor relation and the values extracted from the multiple Coulomb excitation data. Kearns *et al.*[29] have also measured the lifetimes of rotational states in ^{164}Er by the Doppler-broadened line-shape technique using Coulomb excitation with ^{56}Fe and ^{84}Kr projectiles. They found the $B(E2)$ values for decay of the 8^+ and 10^+ states to be in good agreement with rotational values, but their value for the $B(E2; 12^+ \rightarrow 10^+)$ level is more than 32% lower than the rotational prediction and our values derived from both Doppler-broadened line shape and multiple Coulomb excitation yield measurements.

III. DISCUSSION

A. Rotational-alignment model

Since the rotation-alignment model[1] will be used extensively in interpreting the high-spin level structure of ^{164}Er, it is appropriate that we examine the qualitative predictions of this model. A characteristic feature of the rotation-alignment model is that it predicts a series of rotation-aligned bands similar to the superbands observed in ^{164}Er. Calculations within the rotation-alignment model[1,7] predict that the wave functions of the low-lying positive-parity two-quasiparticle bands in nuclei such as ^{164}Er are dominated by a single K component at low spin ($I \leq 4$) and one rotation-aligned structure for $I^\pi \geq 16^+$. The lowest yrast even-spin rotation-aligned band has only even-spin members and evolves from a $K^\pi = 0^+$ structure (at spin zero) to a structure at $I \geq 16$ which is mainly two $i_{13/2}$ quasineutrons coupled to $J = 12$ and aligned with the rotation of the core. This is presumed to be the superband observed to intersect the ground-state band at $I^\pi = 16^+$ in ^{164}Er, producing the well-known backbend in the yrast sequence. The next two lowest bands are predicted to start out as a single $K^\pi = 4^+$ band which evolves into the lowest odd-spin (yrast odd) and the second-lowest even-spin (yrare even) rotation-aligned bands. The largest components of the wave functions of these two bands for $I^\pi > 16^+$ have a rotation-aligned structure with two $i_{13/2}$ neutrons coupled to $J = 12$ and $J = 10$ for the odd- and even-spin bands, respectively. The odd-even splitting for the yrast superbands occurs because both R (the core rotation) and J (spin of the two coupled neutrons) are only even, whereas the total spin $\vec{I} = \vec{R} + \vec{J}$ can be both even or odd; thus the rotational energy of an odd-spin state is similar to the next higher even-spin state. The yrare even-spin superband is predicted to be slightly above the yrast odd-spin aligned band, and it has a structure for which roughly half of the wave function corresponds to the two $i_{13/2}$ neutrons coupled to $J = 10$ with maximum alignment along the rotation axis. In the extreme limit of the rotation-alignment model, the yrast even-spin (I), yrast odd-spin ($I-1$), and yrare even-spin ($I-2$) states would have the same rotational energy, because they have the same value of R.

The structure of these rotation-aligned superbands can be probed by studying the interaction of these bands with the ground-state band and with the β- and γ-vibrational bands. The interaction of the lowest superband with the ground and β bands

has been observed previously.[30-37] The interaction matrix elements between the ground-state band and this superband lie between 8 and 80 keV, which is one to two orders of magnitude smaller than typical Coriolis matrix elements at this spin.[38] The interaction between the β band and the lowest superband is known to be weak; that is, it is around 30 keV and 55 keV for ^{154}Gd and ^{156}Dy, respectively,[32,33,38] at the band intersections. The γ band would appear to serve as a better probe of the superbands, since one can study the interactions with both even- and odd-spin states of the superbands, if the necessary intersections of these bands with the γ band can be observed. On the other hand, the ground-state and β bands can only probe the even-spin states. Prior to our previous publication[6] in which we presented evidence for the discovery of the yrast odd- and yrare even-spin superbands, only the lowest superband (yrast even-spin) had been observed and the intersection of superbands with the γ band had never been observed.

B. Backbending of positive-parity bands

The plot of the experimental energies versus spin [Fig. 10(a)] clearly shows that several intersecting bands exist in ^{164}Er. These results can be understood when compared with the predictions of the rotation-alignment model.[1] A sample calculation was performed within this model to illustrate the general features predicted by the model, but no attempt was made to fit the calculation to the experimental data. Both zero and two-quasineutron configurations within the complete $i_{13/2}$ orbit were included. The Fermi level was taken to be between the $\Omega=\frac{3}{2}$ and $\frac{5}{2}$ orbitals with the pairing parameter $\Delta=1$ MeV. A common moment of inertia parameter $2\mathcal{I}/\hbar^2=78.1$ MeV^{-1} was used throughout the calculations except that the ground-band energies were allowed to follow a typical VMI (Ref. 39) behavior. The excitation energies predicted by this calculation are compared with the experimental results in Fig. 10. The γ band was not explicitly included in the calculations; however, a line corresponding to the expected position of the γ-vibrational band in ^{164}Er has been added to Fig. 10 for illustration. The overall similarity between the experimental data and the calculation is striking. The lowest two-neutron band is expected to intersect the γ band between spin 12^+ and 14^+ and the ground band near spin 16^+. The yrare even-spin and yrast odd-spin two-neutron bands are expected to intersect the γ band around spin 15^+. The yrast odd-spin two-quasineutron band is predicted to be about 0.5 MeV above the yrast even-spin rotation-aligned band and it also is predicted to fall slightly below the yrare even-spin rotation-aligned band.

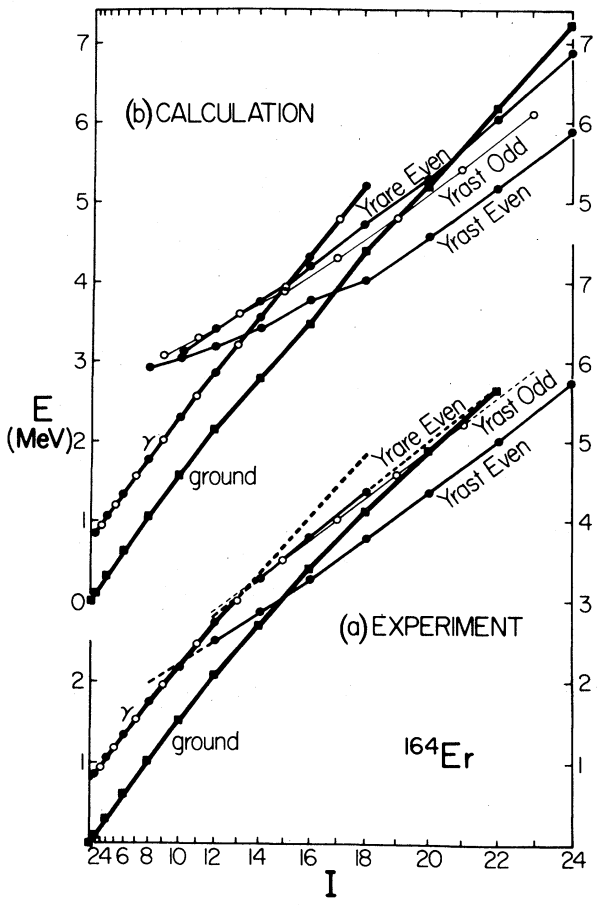

FIG. 10. Plot of the level excitation energies for various bands in ^{164}Er from (a) experiment and (b) the rotation-alignment model. The solid circles correspond to even-spin states and the open circles to odd-spin states.

All of the predicted features appear to be exhibited by the data. The calculation predicts that the ground-state band will intersect the yrare even-spin band and an extrapolation of the experimental third 16^+ and 18^+ states to higher spin suggests such an intersection with the ground band will occur experimentally near spin 24^+. A more detailed comparison shows that the calculations are inadequate in that the intersections are predicted to occur at spins which are slightly too high. In addition, even though the calculation predicts small interaction matrix elements between the intersecting bands, the predicted matrix elements appear to be around a factor of 3 larger than experimentally observed. Almberger *et al.*[40] performed a similar calculation in which they made a least square fit to the experimental level energies to determine four parameters—the Fermi level, the pairing gap, and the magnitude

and slope of the moment-of-inertia dependence of rotational frequency. Using reasonable values for these parameters, they obtained excellent fits, i.e., a rms deviation of only 4 keV, for both the ground band and the yrast superband.

The interaction between the intersecting bands is most clearly illustrated by a conventional backbending plot as shown in Fig. 11. The backbending behavior of the ground-state band of ^{164}Er is very similar to that observed[41] in the other $N=96$ isotopes ^{166}Yb, ^{168}Hf, and ^{170}W. The yrast superband displays about the same moment of inertia and excitation energy in all of these nuclei. Below the backbend the moment of inertia characteristically increases slightly with increasing spin, presumably due to the influence of Coriolis antipairing. If it is assumed that the backbending in the yrast even-spin sequence is due to the intersection of two bands with an interband interaction strength of 45 keV, then the unperturbed ground-band states lie on a smooth extension of the lines up through the 18^+ state, and the yrast even-spin superband energies vary smoothly as shown by the open circles in the left portion of Fig. 11. However, the 20^+ and 22^+ members of the ground band are affected very little by this interaction. We note that if we extrapolate the yrare-even superband, as shown by the dashed line in Fig. 10(a), and assume that the interaction between these bands is 45 keV, then the upward kink in the ground band for the 20^+ and 22^+ states is largely removed.

The ratio of the intraband and interband $B(E2)$ values at the band intersection is sensitive to the strength of the interaction between the intersecting bands. The interaction strength can be determined from the measured branching ratio, provided the level energies are known, if it is assumed that only two bands are interacting and that the bands have the same intrinsic quadrupole moments. The γ-ray branching ratio $16^{+\prime}\rightarrow 14^{+\prime}/16^{+\prime}\rightarrow 14^{+}=0.22\pm 0.07$ implies an interaction strength between the ground band and yrast even-spin superband of $B_c=51^{+2}_{-6}$ keV. Kistner *et al.*[8] obtain a value of 0.40 for this branching ratio, implying an interaction strength of 43 keV. These values are consistent with the 45-keV interaction strength implied by the perturbation of the level energies. The absolute $B(E2)$ values measured by multiple Coulomb excitation also are consistent with the 45-keV interaction strength as illustrated in Fig. 7. The $B(E2;14^{+\prime}\rightarrow 12^{+})$ can be inferred from the γ-ray branching ratio $14^{+\prime}\rightarrow 12^{+}/14^{+\prime}\rightarrow 12^{+\prime}$ assuming that the superband has a constant intrinsic quadrupole moment similar to the ground band. This $B(E2;14^{+\prime}\rightarrow 12^{+})$, shown by an open circle in Fig. 7, is in good agreement with the value (dashed line) predicted assuming a 45-keV interaction between the intersecting bands.

Gamma-ray branching ratios at the backbend have been measured[32,33] in two other nuclei, ^{154}Gd and ^{156}Dy. Average interaction matrix elements of 23.5 ± 1.5 keV for the 16^+ and 18^+ states in ^{154}Gd and 8.5 ± 1.5 keV for the 16^+ state in ^{156}Dy result from similar calculations. Band-interaction matrix elements of this size are remarkably small, i.e., they are nearly two orders of magnitude smaller than expected for Coriolis matrix elements at these spins, but are consistent with the rotation-alignment model.

Calculations[1,7] within the two-quasiparticle-plus-rotor model show that the aligned two $i_{13/2}$ neutron eigenfunctions for the yrast states become localized around $J=12$ and $R=I-12$ with increasing spin. On the other hand, the zero-quasiparticle ground band has $I=R$ for a fully paired state. The Coriolis force does not couple states with differing core rotation R, and thus the two bands interact only via the overlap of weak components in the wave functions. This overlap becomes progressively smaller with increasing spin due to the increased localization in R space of the aligned states. Calculations[1,4,7] within this model suggest that the interaction is ≤ 140 keV and is nearly constant for $10<I<22$. Although these calculations predict small interaction matrix elements, they are still more than a factor of 2 or 3 larger than experimental values. This implies that the assumptions made in these calculations may not be completely adequate. A more complete Hartree-Fock-Bogoliubov calculation by Mang[42] also predicts small interaction strengths.

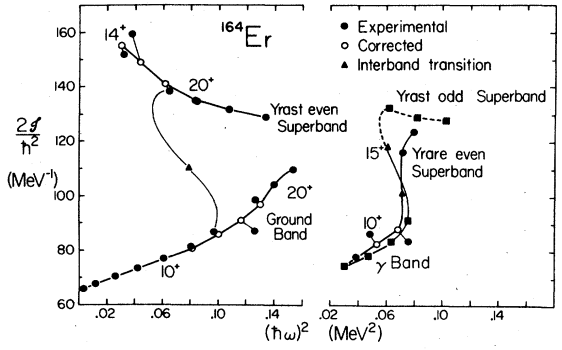

FIG. 11. Plot of $2\mathcal{I}/\hbar^2$ versus $(\hbar\omega)^2$ for members of the ground-state band, γ-vibrational band, and superbands in ^{164}Er. The open circles on the ground-state and even-yrast superbands are corrections for a 45-keV interaction matrix element. The energies of the 10^+_γ and 12^+_γ states were adjusted in accord with this interaction strength. The circles represent even-spin and the squares odd-spin states.

A backbending plot for the transitions in the γ-vibrational band of ^{164}Er is shown on the right side of Fig. 11. The rotation-alignment model suggests that the interaction between the lowest rotation-aligned two-neutron bands and the ground-state, β and γ bands will be weak and of comparable strength. As a first approximation, we assumed that the three superbands have the same interaction strength of 45 keV with both the ground-state and γ bands. Furthermore, we assumed that we could estimate the positions of unobserved states by making the extrapolations shown by dashed lines in Fig. 10. The positions of the unperturbed levels were then calculated and are plotted as open circles in Fig. 11. This procedure produces a 25-keV shift in the 10^+_γ level energy and equal but opposite shifts in the $10^+_\gamma \rightarrow 8^+_\gamma$ and $12^+_\gamma \rightarrow 10^+_\gamma$ transition energies. The obvious discontinuities in the backbending plot for the even-I members of the γ band are removed if the unperturbed values are used. The odd-spin state energies in the γ band are smooth in this spin region without such a shift. The behavior of the odd-spin sequence provides direct evidence that the odd-spin states in the yrast superband lie considerably higher than the even-spin states.

The abrupt backbends of both the even- and odd-spin sequences of the γ band are apparent around spins 13 and 14. Even without the placements of the tentative 17^+ and higher-spin states, it is also apparent that a marked reversal in the odd-even staggering occurs through the backbend region. This behavior becomes more obvious when the states of the γ band (and the superband continuation) are displayed as in Fig. 12, where it is clear that the odd-spin states lie low relative to the even-spin ones below the backbend and high after the backbend. There is also the possibility that the behavior in the (true) γ band below the backbend is caused by the interaction with the β band which lies 400 keV above the γ band. An interaction of about 100 keV between these bands could reproduce the observed odd-even staggering just below the backbend. However, the higher-spin states of the γ band give the best insight into this situation. Above the backbend the rotation-alignment model predicts both the behavior in the odd-even staggering and the relative moments of inertia of the yrare even-I and yrast odd-I superbands (89 and 96%, respectively, of the yrast even-I superband moment of inertia at similar spin values). The observed reversal in the staggering is the strongest evidence that these higher superbands correspond to the higher $i_{13/2}$ bands coupled to the ground band.

The γ-ray branching ratios at the band intersections with the γ band also can be used to determine

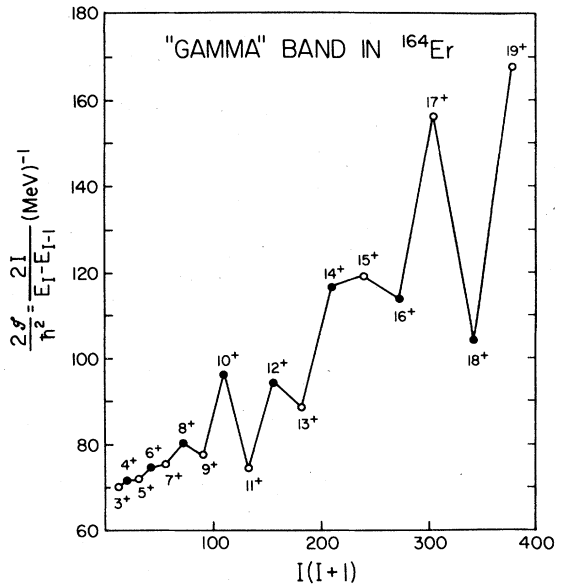

FIG. 12. Plot of $2I/(E_I - E_{I-1})$ versus $I(I+1)$ for the γ-vibrational band in ^{164}Er. The odd-even staggering as well as a change in this effect at higher spins is clearly shown.

the interaction strength. The absence of observed superband states below the intersection with the γ band can be understood if the interaction matrix element is 45 keV. Both the yrast and yrare even-I superbands are then predicted to decay 85% into the γ band at the intersection, while the odd-I superband is calculated to have a 77% branch into the γ band. Thus in all three cases the lower superband branch would be too weak to be observed in our work. The $B(E2; 10^+_\gamma \rightarrow 12^+_\gamma)$ and $B(E2; 12^+_\gamma \rightarrow 14^+_\gamma)$ values will be attenuated by about 50% assuming band mixing with a 45-keV interaction strength. The experimental $B(E2)$ values shown in Fig. 8 are of insufficient accuracy to determine whether this attenuation occurs.

The energy separation between the γ and ground bands is similar to the separation between the upper two superbands and the lowest superband. This suggests a second possible explanation[6,43,44] for the structure of the two upper superbands, i.e., they could be composed of the lowest $i_{13/2}$ yrast superband coupled to the γ band. However, it is not apparent to us that this model can explain the change in the odd-even staggering observed at the backbend.

The calculations show that the splitting between the yrast even-spin (I), the yrast odd-spin ($I-1$), and the yrare even-spin ($I-2$) two-quasiparticle bands is proportional to I at low spin, where a given K value dominates the wave function and then becomes constant when a rotation-aligned

configuration dominates. If it is assumed that the three observed superbands are indeed two-quasiparticle rotation-aligned bands, as suggested by the present data, then the spin at which these splittings become approximately constant with I can be used as a check on the Coriolis matrix elements. Almberger *et al.*[40] used these data to determine if a Coriolis attenuation factor is required in two-quasiparticle-plus-rotor calculations. They determined the attenuation factor to be 0.97, i.e., essentially no attentuation, in agreement with the earlier conclusions of Flaum and Cline.[7] This result is to be compared with values from 0.60 to 0.76 required in one-quasiparticle-plus-rotor descriptions of positive-parity states in neighboring odd-neutron nuclei.[45,46]

C. Negative-parity bands

The yrast (5^-) and yrare (7^-) negative-parity bands have been interpreted[13] as rotational bands built on the $\{\frac{5}{2}^-[523]\nu;\frac{5}{2}^+[642]\nu\}_5$- and $\{\frac{7}{2}^+[404]\pi;\frac{7}{2}^-[523]\pi\}_7$- two-quasiparticle configurations. The moments of inertia for these bands derived from the $E_I - E_{I-1}$ level spacing are plotted versus $I(I+1)$ in Fig. 13. The 5^- band exhibits (1) an odd-even staggering which reverses sign at spin 21^-, (2) a moment of inertia comparable to those of the positive-parity superbands, i.e., close to the rigid body value, (3) a moment of inertia which decreases with increasing spin at low-spin values, (4) intraband γ-decay paths which separate into an odd-spin sequence and an even-spin sequence, and (5) $E1$ transitions from the odd-spin states to the ground band which occur with inhibition factors

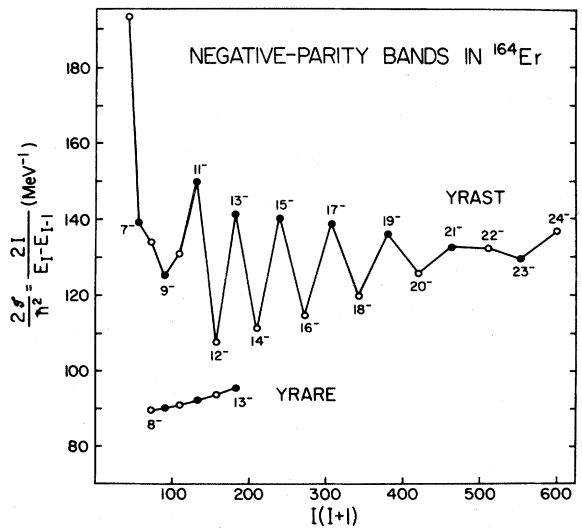

FIG. 13. Plot of $2I/(E_I - E_{I-1})$ versus $I(I+1)$ for the negative-parity states in ^{164}Er.

of $\sim 10^4$ relative to the Weisskopf estimate. These features suggest that rotation alignment is important for this band. Similar features have been observed[30] in negative-parity bands in ^{126,128}Ba. In contrast, the 7^- band exhibits a moment of inertia which increases smoothly from 60% to 64% of the rigid-body value as the spin increases from 8^- to 13^- and $E1$ transitions are inhibited by factors of $\sim 5\times 10^9$ relative to the Weisskopf estimate. These are characteristic of a deformation-aligned band with a relatively good K quantum number.

The behavior observed in these negative-parity bands was predicted by the two-quasiparticle-plus-rotor model calculations of Flaum and Cline.[7] These calculations, which were made for both positive- and negative-parity bands in ^{156}Er, showed that the structure of the yrast negative-parity band above spin 11^- was characterized by the $[\nu h_{9/2}, \nu i_{13/2}]J^\pi = 11^-$ rotation-aligned two-quasiparticle configuration. States with $I^\pi \leq 11^-$ were strongly influenced by collective 3^-, 5^-, etc. correlations because the residual two-quasiparticle interaction is comparable to the Coriolis interaction for these low-spin values. The rotation-aligned band was predicted[7] to exhibit a large odd-even staggering in excitation energy. The reason for this behavior is that the angular momentum of the core, R, has only even-spin values for axial symmetry. Consequently, since the total spin $\vec{I}=\vec{R}+\vec{J}$ (J is the angular momentum of the two quasiparticles), it follows that for J odd (even) the odd (even) spin, $|I| = |R| + |J|$ (fully aligned) and $I' = I - 1$ (partially aligned) states will have the same value of R and hence the same rotational energy. Thus, since the $[\nu h_{9/2}, \nu i_{13/2}]J^\pi = 11^-$ two-quasiparticle configuration is predicted to dominate the structure of the yrast negative-parity band, then the I^-_{odd} and $I^-_{\text{odd}} - 1$ states will be nearly degenerate in excitation energy when rotation alignment is complete. Flaum and Cline[7] predicted that at high-spin values the $[\nu h_{11/2}, \nu i_{13/2}]J^\pi = 12^-$, two-quasiparticle configurations will start to dominate the wave function and then the I^-_{even} states will be depressed in energy relative to the I^-_{odd} states. That is, a reversal in the odd-even staggering should occur at high spin.

The rotation-aligned configurations are predicted to dominate the wave function of the yrast negative-parity band in ^{156}Er because the Fermi level is close to the $\Omega = \frac{1}{2}$ orbitals based on $\nu i_{13/2}$ and $\nu h_{9/2}$ spherical shell model configurations. Two-quasiparticle-plus-rotor model calculations were not performed for the negative-parity states in ^{164}Er, but what will occur in ^{164}Er is clear by reference to the calculations[7] for ^{156}Er. The Fermi level in ^{164}Er is close to the $\Omega = \frac{5}{2}$ orbitals

based on $\nu i_{13/2}$ and $\nu h_{9/2}$ spherical shell model configurations; consequently, the rotation alignment should be appreciably less complete than for ^{156}Er. This is what is observed. The I^{-}_{odd} states are depressed in energy relative to the I^{-}_{even} states, but the effect is appreciably smaller than predicted for ^{156}Er. The data also exhibit the large moments of inertia and the reversal in odd-even staggering at $I^{\pi}=21^{-}$, both of which are expected for rotation-aligned two-quasiparticle configurations.

The calculations[7] for ^{156}Er show that rotation alignment is unimportant for the lowest two-proton negative-parity band because of the j and high Ω of the important configurations (i.e., $\frac{7}{2}^{+}[404]$ and $\frac{7}{2}^{-}[523]$). Consequently, this band should have a smaller moment of inertia and no noticeable odd-even staggering at lower-spin values. This is exactly what is observed for the 7^{-} band in ^{164}Er. Since K is a good quantum number, the $E1$ decay to the ground band will be strongly inhibited as is observed.

Bengtsson and Frauendorf[44] have also performed a detailed theoretical analysis of the observed bands in ^{164}Er. They analyze the energies of the bands in the rotating frame of the nucleus and compare these to the results of cranking model calculations. This comparison leads to quasiparticle assignments for the yrast (5^{-}) and yrare (7^{-}) negative-parity bands identical, at least at lower spins, to those indicated by the rotation-alignment calculations discussed in the present paper. Furthermore, Bengtsson and Frauendorf[44] suggest the $\{\frac{11}{2}^{-}[505]\nu;\frac{5}{2}^{+}[642]\nu\}_{8^{-}}$ interpretation for the band beginning with $I=8$ at 2090.9 keV, an assignment which our rotation alignment calculations indicate may become important in the composition of the 5^{-} band at higher spins, as discussed above.

IV. SUMMARY

A relatively complete description of the high-spin states of ^{164}Er has emerged from the present work. Several positive-parity and two negative-parity bands have been identified. The previously reported backbending behavior of the positive-parity yrast sequence is demonstrated to result from the intersection of the ground band, seen to spin 22^{+}, with an even-spin "superband," having a large moment of inertia, which is observed from spins 12^{+} to 24^{+}. The observed interaction between this yrast superband and the γ band demonstrates that this band possesses only even-spin members for $I \geq 12^{+}$. We have found additional even-spin (yrare even) and odd-spin (yrast odd) superbands possessing large moments of inertia which lie about 0.5 MeV above the lowest superband. The interaction of these bands with the γ band was observed. Although the evidence is weak, the data also imply that the ground-state and yrare even-spin bands intersect at $I \approx 24$. The observed level energies and γ-ray branchings are consistent with the three superbands having a constant 45 keV interaction matrix element with the ground-state and γ bands. These interaction matrix elements are more than an order of magnitude smaller than typical Coriolis matrix elements at these spin values. The level energies of the two negative-parity bands are observed to behave differently; the 7^{-} band behaves like a good rotor while the 5^{-} band exhibits an odd-even staggering characteristic of a rotation-aligned band.[1,7]

The Coulomb excitation and lifetime data are all consistent with a picture of interacting rotational bands with an interaction matrix element $\approx$45 keV. In particular, the $B(E2)$ values for the unperturbed ground band are in agreement with the rigid-rotor relation, i.e., with a constant intrinsic quadrupole moment, while the excitation of the γ band is consistent with the prediction of the rigid-triaxial-rotor model with asymmetry $\gamma=12.7°$.

The rotation-alignment model successfully explains the available data and correctly predicts the occurrence and relative energies of the superbands when typical collective model parameters are assumed. Moreover, it gives approximately the correct spin for the intersection of these three bands with the ground-state and γ bands. This model predicts the relative moments of inertia of all the intersecting bands and, in particular, correctly accounts for the reversal in the odd-even staggering at the backbend in the γ band. The model also reproduces the very different moments of inertia and odd-even staggering behavior of the 5^{-} and 7^{-} bands. This model is consistent with the observed $E2$ properties. The rotation-alignment model also predicts very small interaction matrix elements between the intersecting bands although not quite as small as the observed values. All of the evidence strongly supports the rotation-alignment model description of the structure of the superbands in ^{164}Er.

It should be pointed out that, although the rotation alignment and cranking models take somewhat different approaches to explain the backbending phenomenon, they both predict very similar band crossing properties and represent the same underlying physics.

ACKNOWLEDGMENTS

We are indebted to the operating crew of the SuperHILAC and the ORIC operations staff for

their help during these experiments. This research was supported in part by the U.S. Department of Energy, partially under contract with Union Carbide Corporation, and by the National Science Foundation. One of us (E.L.R.) wishes to thank the University of Alabama (Birmingham) Graduate Faculty Research Committee for partial support of his participation in this research.

---

*Also at Lawrence Berkeley Laboratory, Berkeley, California 94720.
†Deceased.
‡Present address: Cyclotron Institute, Texas A & M University, College Station, Texas 77843.
§Present address: Gesellschaft für Schwerionenforschung, Darmstadt, Germany.
‖Present address: Department of Physics, University of Liverpool, P. O. Box 147, Liverpool L69 3BX, United Kingdom.
¶Present address: Etudes et Productions, Schlumberger, 25 Rue de la Cavée, 92142 Clamart, France.
**Present address: Cyclotron Laboratory, Michigan State University, East Lansing, Michigan 48824.
††Present address: Department of Radiology, Medical Physics, University Hospitals, Madison, Wisconsin 53706.

[1]F. S. Stephens and R. S. Simon, Nucl. Phys. A183, 257 (1972).
[2]F. S. Stephens, Rev. Mod. Phys. 47, 43 (1975).
[3]B. R. Mottelson and J. G. Valatin, Phys. Rev. Lett. 5, 511 (1960).
[4]I. Y. Lee, D. Cline, R. S. Simon, P. A. Butler, P. Colombani, M. W. Guidry, F. S. Stephens, R. M. Diamond, N. R. Johnson, and E. Eichler, Phys. Rev. Lett. 37, 420 (1976).
[5]N. R. Johnson, S. W. Yates, R. M. Ronningen, R. D. Hichwa, L. L. Riedinger, and A. C. Kahler, Bull. Am. Phys. Soc. 21, 984 (1976) and Proceedings of the International Conference on Nuclear Structure, Tokyo, 1977, edited by T. Marumori (Physical Society of Japan, Tokyo, 1978).
[6]N. R. Johnson, D. Cline, S. W. Yates, F. S. Stephens, L. L. Riedinger, and R. M. Ronningen, Phys. Rev. Lett. 40, 151 (1978).
[7]C. Flaum and D. Cline, Phys. Rev. C 14, 1224 (1976).
[8]O. C. Kistner, A. W. Sunyar, and E. der Mateosian, Phys. Rev. C 17, 1417 (1978).
[9]M. J. Saltmarsh (unpublished).
[10]M. L. Halbert (unpublished).
[11]M. V. Banaschik, C. Günther, H. Hübel, A. C. Rester, G. Nowicki, and J. J. Pinajian, Nucl. Phys. A222, 459 (1974).
[12]W. F. Davidson, R. M. Lieder, H. Beuscher, A. Neskakis, G. A. Varley, J. C. Willmott, F. Kearns, and J. C. Lisle, J. Phys. G 3, 199 (1976).
[13]F. W. N. de Boer, P. F. A. Goudsmit, P. Koldewijn, and G. J. Meijer, Nucl. Phys. A169, 577 (1971).
[14]R. Graetzer, G. B. Hagemann, K. A. Hagemann, and B. Elbek, Nucl. Phys. 76, 1 (1966).
[15]R. L. West, E. G. Funk, A. Visvanathan, J. P. Adams, and J. W. Milhelich, Nucl. Phys. A270, 300 (1976).
[16]J. H. Jett and D. A. Lind, Nucl. Phys. A155, 182 (1970).
[17]D. Elmore, Ph.D. thesis, University of Rochester, 1974.
[18]A. Winther and J. de Boer, in *Coulomb Excitation*, edited by K. Adler and A. Winther (Academic, New York, 1966), p. 303.
[19]R. M. Ronningen, R. B. Piercey, J. H. Hamilton, C. F. Maguire, A. V. Ramayya, H. Kawakami, B. van Nooijen, R. S. Grantham, W. K. Dagenhart, and L. L. Riedinger, Phys. Rev. C 16, 2218 (1977).
[20]R. Brenn, H. Spehl, A. Wecherlin, H. Doubt, and G. van Middlekoop, Z. Phys. A281, 219 (1977).
[21]M. W. Guidry, P. A. Butler, R. Donagelo, E. Grosse, Y. El Masri, I. Y. Lee, F. S. Stephens, R. M. Diamond, L. L. Riedinger, C. R. Bingham, A. C. Kahler, J. A. Vrba, E. L. Robinson, and N. R. Johnson, Phys. Rev. Lett. 40, 1016 (1978).
[22]D. Cline, Nukleonika (to be published).
[23]W. T. Milner (unpublished).
[24]L. C. Northcliffe and R. F. Schilling, Nucl. Data Tables A7, 23 (1970).
[25]J. F Ziegler and W. K. Chu, At. Data Nucl. Data Tables 13, 463 (1974).
[26]M. W. Guidry, P. A. Butler, P. Colombani, I. Y. Lee, D. Ward, R. M. Diamond, F. S. Stephens, E. Eichler, N. R. Johnson, and R. Sturm, Nucl. Phys. A266, 228 (1976).
[27]J. Lindhard, M. Scharff, and H. E. Schiott, K. Dan. Vidensk. Selsk, Mat. Fys. Medd. 33, no. 14 (1963).
[28]A. E. Blaugrund, Nucl. Phys. 88, 501 (1966).
[29]F. Kearns, G. Varley, G. D. Dracoulis, T. Inamura, J. C. Lisle, and J. C. Willmott, Nucl. Phys. A278, 109 (1977).
[30]C. Flaum, D. Cline, A. W. Sunyar, and O. C. Kistner, Phys. Rev. Lett. 33, 973 (1974); Nucl. Phys. A264, 291 (1976).
[31]R. A. Warner, F. M. Bernthal, J. S. Boyno, T. L. Khoo, and G. Sletten, Phys. Rev. Lett. 31, 835 (1973).
[32]T. L. Khoo, F. M. Bernthal, J. S. Boyno, and R. A. Warner, Phys. Rev. Lett. 31, 1146 (1973).
[33]H. R. Andrews, D. Ward, R. L. Graham, and J. S. Geiger, Nucl. Phys. A219, 141 (1974).
[34]R. Lieder, H. Beuscher, W. F. Davidson, A. Neskakis, C. Mayer-Böricke, Y. El Masri, P. Monseu, J. Steyaert, and J. Vervier, Phys. Lett. 49B, 161 (1974).
[35]Y. El Masri, R. Janssens, C. Michel, P. Monseu, J. Steyaert, and J. Vervier, Z. Phys. A274, 113 (1975).
[36]M. Piiparinen, J. C. Cunnane, P. J. Daly, C. L. Dors, F. M. Bernthal, and T. L. Khoo, Phys. Rev. Lett. 34, 1110 (1975).
[37]L. Funke, P. Kemnitz, G. Winter, S. A. Hjorth, A. Johnson, and T. Lindblad, Phys. Lett. 55B, 436 (1975).
[38]D. Cline, Bull. Am. Phys. Soc. 21, 962 (1976).
[39]M. A. J. Mariscotti, G. Scharff-Goldhaber, and B. Buck, Phys. Rev. 178, 1864 (1969).
[40]J. Almburger, I. Hamamoto, and G. Leander, Nucl. Phys. A333, 184 (1980).

[41]R. O. Sayer, J. S. Smith III, and W. T. Milner, At. Data Nucl. Data Tables 15, 85 (1975).
[42]H. J. Mang, private communication, and J. L. Egido, H. J. Mang, and P. Ring, Nucl. Phys. A334, 1 (1980).
[43]L. K. Peker, private communication.
[44]R. Bengtsson and S. Frauendorf, Nucl. Phys. A314, 27 (1979).
[45]S. A. Hjorth, H. Ryde, K. A. Hagemann, G. Lövhöiden, and J. C. Waddington, Nucl. Phys. A144, 513 (1970).
[46]G. Lövhöiden, P. O. Tjom, and L. O. Edvardson, Nucl. Phys. A194, 463 (1972).
[47]I. Ben-Zvi, A. E. Blaugrund, Y. Dar, G. Goldring, J. Hess, M. W. Sachs, E. Z. Skurnik, and Y. Wolfson, Nucl. Phys. A117, 625 (1968).